Chapter 5

Thermohydraulic and TEG performance analysis with dissimilar shape-based hybrid nanofluids

Overview: This chapter explores how different nanoparticle shapes affect the cooling performance of a mini channel heat sink used to enhance the cold side of a thermoelectric generator (TEG). The study focuses on a 50:50 mixture of hybrid nanofluids containing various nanoparticles: graphene (platelet-shaped), Al_2O_3 (blade-shaped), MWCNT (cylindrical-shaped), and Fe_3O_4 (brick-shaped). The investigation considers different coolant flow rates and nanoparticle concentrations (0.1–1%). Important performance factors analyzed include heat transfer efficiency, Nusselt number, exergy at the inlet and outlet of the heat sink, cooling system efficiency (coefficient of performance, Figure of merit), and the overall impact on TEG power output and efficiency. Water is used as a reference coolant for comparison. The goal is to determine the best hybrid nanofluid composition that improves TEG performance by enhancing heat dissipation.

5.1 Mathematical Modeling

5.1.1 Design of Mini channel Heat Sink

Figs. 5.1 (a), (b), and (c) show the schematic of the overall system and the mini channel heatsink that has been investigated in the study. Copper has been chosen as the material of the MCHS because of its high thermal conductivity. The MCHS has a base area of 30mm X 20mm with nine parallel rectangular channels. The channel width and the channel height are 1mm and 3mm respectively.

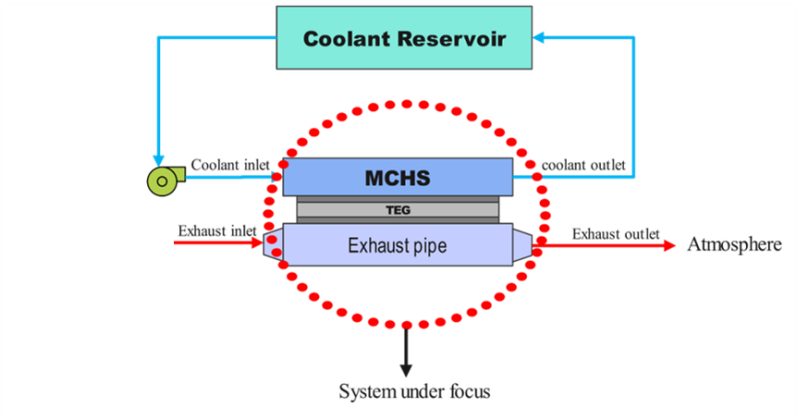

(a)

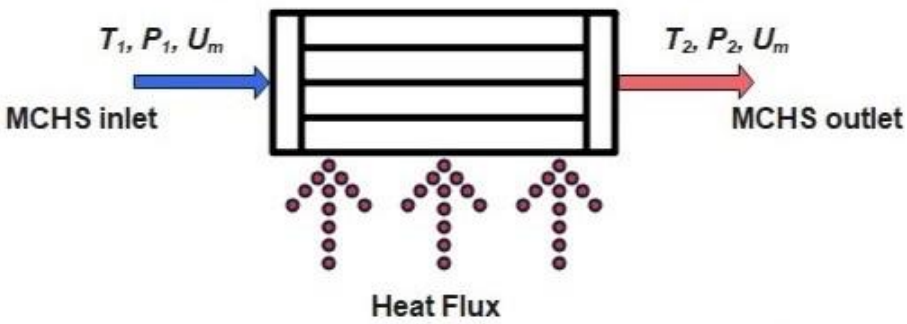

(b)

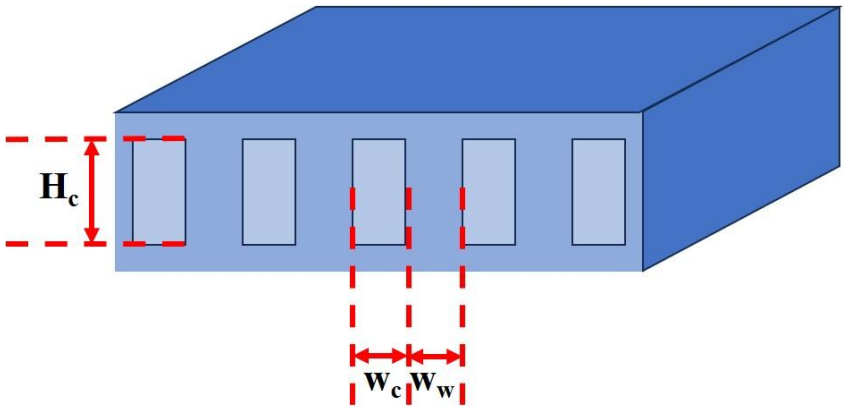

(c)

Fig. 5.1 (a) Schematic diagram of the overall system, (b) MCHS used, and (c) schematic showing MCHS dimensions

The various design variables that have been used for the numerical analysis are defined as (Shamsuddin et al., 2021):

$$\gamma = \frac{H_c}{w_c} \tag{5.1}$$

$$\beta = \frac{w_w}{w_c} \tag{5.2}$$

$$D_h = \frac{2H_c w_c}{H_c + w_c} \tag{5.3}$$

Where γ, β, and D_h denote the MCHS aspect ratio, the width ratio, and the hydraulic diameter respectively. Other important geometric parameters of the MCHS are calculated below:

$$A_c = H_c w_c \tag{5.4}$$

$$W = n(w_c + w_w) \tag{5.5}$$

$$\gamma_{inv} = \frac{1}{\gamma} \tag{5.6}$$

5.1.2 Boundary Conditions

Uniform velocity and temperature have been assumed at the inlet. The coolants (water and hybrid nanofluid of different shapes i.e., graphene-platelet shape, Al_2O_3-blade shape, MWCNT-cylindrical shape, and Fe_3O_4-brick shape) are incompressible, Newtonian, and no-slip boundary condition applies at the MCHS walls (Kumar and Sarkar, 2019). The MCHS is identical in both heat transfer and hydrodynamics. The remaining walls have been considered adiabatic. Also, the numerical analysis is done by treating the flow as steady-state, and single phase. The range of volume flow rate considered renders laminar flow because of the low value of the hydraulic diameter of the MCHS (Tuckerman and Pease, 1981). Heat rejected from the exhaust gas is equal to the heat gained by the hot side of TEG. Heat transfer due to thermal radiation is neglected. The contact resistances between the TEG - exhaust gas and TEG - coolant are neglected. Heat transfer in the ducts is neglected.

5.1.3 Fluid flow correlations

The commonly used flow parameters are calculated below:

$$\dot{m} = \rho n A_c U_m \tag{5.7}$$

$$\dot{V} = \frac{\dot{m}}{\rho} \tag{5.8}$$

$$Re = \frac{\rho U_m D_h}{\mu} \tag{5.9}$$

The pressure drop across the channel is accounted for by the following relations (Shamsuddin et al., 2021):

$$\Delta P = \Delta P_{laminar} + \Delta P_{constriction\ and\ expansion} \tag{5.10}$$

Where the individual pressure drop terms have been defined as:

$$\Delta P_{laminar} = \frac{f_{app}\rho U_m^2}{2}\left(\frac{1+\gamma}{2\gamma}\right) + \frac{\rho U_m^2}{2}\left(1.8 - \left(\frac{2.4}{1+\beta}\right) + \left(\frac{0.6}{1+\beta}\right)\right) \tag{5.11}$$

$$\Delta P_{constriction\ and\ expansion} = \frac{\rho U_m^2}{2}\left(1.79 - \left(\frac{2.32}{1+\beta}\right) + \left(\frac{0.53}{1+\beta}\right)\right) \tag{5.12}$$

$$f_{app} = \frac{\left[\left\{3.2\left(Re\frac{D_h}{L}\right)^{0.52}\right\}^2 + (18.8 + 78.57Be)^2\right]^{0.5}}{Re} \tag{5.13}$$

Where f_{app} is the friction factor that depends on the hydraulic diameter, Reynolds number, length of the mini channel heatsink, and a dimensionless parameter, *Be*, defined by Bejan (2013) as:

$$Be = \frac{\left(1 + \frac{1}{\gamma^2}\right)}{\left(1 + \frac{1}{\gamma}\right)^2} \tag{5.14}$$

Thus, the power consumed in pumping the working fluid is the product of the total pressure drop and the volume flow rate:

$$Power = \Delta P\dot{V} \tag{5.15}$$

5.1.4 Heat transfer correlations

The capacitive heat transfer by the exhaust and the coolant during flow through and various other heat transfer relations is given as follows:

$$\dot{Q_{ex}} = \dot{m}_{ex} C_{p,ex}(T_{in,ex} - T_{out,ex}) \tag{5.16}$$

$$\dot{Q}_{ex} = h_{ex} SA_{ex}(T_{avg,ex} - T_{pipe}) \tag{5.17}$$

$$\dot{Q}_H = \dot{Q}_{ex}({}^{A_{TEG}}/_{SA_{ex}}) \tag{5.18}$$

$$\dot{Q}_H = (T_{pipe} - T_h)/R_{cond} \tag{5.19}$$

$$\dot{Q}_H = N(\alpha I T_H + k(T_H - T_L) + {}^{I^2R}/_{2}) \tag{5.20}$$

$$\dot{Q}_L = N(\alpha I T_H + k(T_H - T_L) - {}^{I^2R}/_{2}) \tag{5.21}$$

$$\dot{Q}_L = \dot{m}_c C_{p,c}(T_{out} - T_{in}) \tag{5.22}$$

For the calculation of the Nusselt number, the following correlations have been used (Bejan, 2013):

$$x^* = \frac{L}{D_h Re Pr} \tag{5.23}$$

$$Nu = 1.87(x^*)^{-0.3} {\gamma_{inv}}^{-0.056} Pr^{-0.036} \tag{5.24}$$

$$Nu = 3.35(x^*)^{-0.13} {\gamma_{inv}}^{-0.12} Pr^{-0.038} \tag{5.25}$$

$$Nu = \frac{hD_h}{k_f} \tag{5.26}$$

Where x^* is the thermal entry length. The thermal entry length helps choose the Nusselt number correlation which will be used for the calculation of the average heat transfer coefficient. This parameter takes the geometry of the mini channel heatsink as well as the thermophysical properties of the coolant into account, and hence the effect of the shape factor of the various nanoparticles. The following equations are used for

ascertaining the fin efficiency of the walls, the total resistance, and the individual resistances comprising it i.e., conductive, convective, and capacitive resistance (Yang et al., 2017):

$$R_{total=}R_{cond} + R_{conv} + R_{cap} \tag{5.27}$$

$$R_{cond} = \frac{t}{k_w WL} \tag{5.28}$$

$$R_{conv} = \frac{1}{nhL(w_c + 2\eta_{fin}H_c)} \tag{5.29}$$

$$R_{cap} = \frac{1}{\dot{m}c_p} = \frac{1}{n\rho U_m H_c w_c c_p} \tag{5.30}$$

$$\eta_{fin} = \frac{\tanh(mH_c)}{mH_c}, where\ m = \sqrt{\frac{2h}{k_w w_w}} \tag{5.31}$$

Where k_w denotes the thermal conductivity of the MCHS wall and η_{fin} indicates the fin efficiency of the heatsink wall for convection. The heatsink temperature, average fluid temperature, and total heat transfer can be expressed as:

$$T_{hs} - T_{avg} = R_{total}\dot{Q}_L \tag{5.32}$$

$$T_{avg} = \frac{T_{in} + T_{out}}{2} \tag{5.33}$$

Where T_{hs} is the uniform heatsink temperature for the applied heat flux. Also, the coolant reservoir is assumed to be an infinite sink.

5.1.5 Nanoparticles and Nanofluid

Despite their enhanced thermal properties, nanofluids face challenges related to stability, as nanoparticles tend to agglomerate and settle. This can be remedied by using surfactants or surface functionalization. Additionally, their increased viscosity leads to higher pumping power requirements. Optimizing nanoparticle concentration and utilizing non-spherical shapes can help mitigate this pressure drop penalty while maintaining

superior heat transfer. However, nanofluids provide a major advantage: significantly higher thermal conductivity than base fluids, leading to vastly improved heat transfer and cooling efficiency. This allows for the design of more compact thermal systems. Their properties can also be customized for specific applications.

The volume fraction for the hybrid nanofluid is given below where subscripts 1 and 2 denote the dissimilar-shaped nanoparticles according to the blend. The Eqs. incorporate the shape effect of the nanoparticles viz., platelet, blade, brick, and cylindrical into the thermophysical property of thermal conductivity and rheological property of dynamic viscosity (Kumar and Sahoo, 2019) which considers the heat transfer characteristics, micro-convection, and frictional effects.

$$\varphi = \varphi_1 + \varphi_2 \tag{5.34}$$

$$k_{nf,1} = k_{bf}\left(1 + \left(C_{surface,1} + C_{shape,1}\right)\varphi_1\right) \tag{5.35}$$

$$\mu_{nf,1} = \mu_{bf}(1 + A_1\varphi_1 + B_1\varphi_1^2) \tag{5.36}$$

$$k_{nf,2} = k_{bf}\left(1 + \left(C_{surface,2} + C_{shape,2}\right)\varphi_2\right) \tag{5.37}$$

$$\mu_{nf,2} = \mu_{bf}(1 + A_2\varphi_2 + B_2\varphi_2^2) \tag{5.38}$$

The shape and surface influence on the thermal conductivity and viscosity are reported in Tables 5.1 and 5.2, respectively (Kumar and Sahoo, 2019).

Table 5.1: Shape-based nanoparticle thermal conductivity coefficients

Particle Type	Image	Aspect Ratio	C_{shape}	$C_{surface}$
Platelet	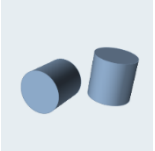	1:1/8	5.72	-3.11

Blade	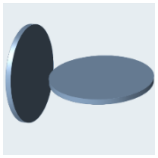	1:6:1/12	8.26	-5.52
Cylindrical	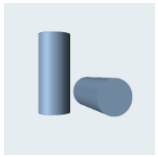	1:8	4.82	-0.87
Brick	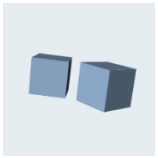	1:1:1	3.71	-0.35

Table 5.2: Shape-based nanoparticle viscosity coefficients

Coefficient	Platelet	Blade	Cylindrical	Brick
A	37.1	14.6	13.5	1.9
B	612.6	123.3	904.4	471.4

The effective thermal conductivity and dynamic viscosity have been calculated using the mixture rule for the dissimilar-shaped nanoparticle hybrid nanofluid (Ramzan et al., 2022):

$$k_{hnf} = \frac{\varphi_1 k_1 + \varphi_2 k_2}{\varphi} \tag{5.39}$$

$$\mu_{hnf} = \frac{\varphi_1 \mu_1 + \varphi_2 \mu_2}{\varphi} \tag{5.40}$$

The effective density and specific heat capacities are expressed below:

$$\rho_{hnf} = \varphi_1 \rho_1 + \varphi_2 \rho_2 + (1 - \varphi)\rho_{bf} \tag{5.41}$$

$$\rho_{hnf} c_{p,hnf} = \varphi_1 \rho_1 c_{p,1} + \varphi_2 \rho_2 c_{p,2} + (1 - \varphi)\rho_{bf} c_{p,bf} \tag{5.42}$$

The properties of the nanoparticles are illustrated in Table 5.3 (Kumar and Sarkar, 2020).

Table 5.3: Nanoparticle thermophysical properties

Particle	ρ, kg/m^3	C_p, J/kgK
Al_2O_3	3970	880
MWCNT	2600	740
Fe_3O_4	5180	670
Graphene	2200	790

The resulting heat transfer and fluid flow properties of the nanofluid are shown in Table 5.4 along with that of water.

Table 5.4: Coolant heat transfer and fluid flow properties

Coolant	k (W/mK)	μ (kg/ms)	Prandtl no.
Water	0.5945	0.0008936	6.287
Plat-blad	0.6025	0.001017	6.889
Plat-cyl	0.6043	0.001024	6.948
Plat-bric	0.6034	0.0009928	6.677
Blad-cyl	0.6045	0.0009678	6.521
Blad-bric	0.6036	0.0009371	6.256
Cyl-bric	0.6054	0.0009433	6.312

5.1.6 Performance parameters

The exergy of a system is the maximum potential work that is possible during heat interaction with the surroundings. Considering negligible changes in the kinetic and the potential energies, the fundamental exergy equations can be written as below (Mahmoud et al., 2021):

$$Ex_{in} = \dot{m}C_p\left[T_{in} - T_{amb} - T_{amb}\ln\left(\frac{T_{in}}{T_{amb}}\right)\right] \tag{5.43}$$

$$Ex_{out} = \dot{m}C_p \left[T_{out} - T_{amb} - T_{amb} \ln\left(\frac{T_{out}}{T_{amb}}\right)\right] \tag{5.44}$$

The coefficient of performance (COP) of a system is the ratio of the desired effect to the power consumed in obtaining it. Thus, the COP of the mini channel heatsink is defined as:

$$COP = \frac{\dot{Q}}{Power} \tag{5.45}$$

The Figure of Merit (FOM) is defined as the ratio of the relative Nusselt number of the hybrid nanofluid to the one-third power of the relative pressure drop of the hybrid nanofluid concerning the base fluid for a given flow rate and volume fraction in the present study. Thus, FOM gives the relative thermal advantage of the fluid over its frictional disadvantage.

$$FOM = \frac{Nu_{hnf}/Nu_{bf}}{\left(\Delta P_{hnf}/\Delta P_{bf}\right)^{1/3}} \tag{5.46}$$

5.1.7 TEG performance

The power generated and the conversion efficiency of the TEG is given as:

$$Power_{TEG} = \dot{Q}_H - \dot{Q}_L \tag{5.47}$$

$$\eta_{conversion} = \frac{Power_{TEG}}{\dot{Q}_H} X\ 100 \tag{5.48}$$

5.2 Validation

The validation process in this study consists of comparing the flow properties of the different mini-channel heat sink models used in the experimental investigation by Tuckerman and Pease (1981) with the current model. The validation is carried out for friction factor and Nusselt number against Reynolds number. The same trend is observed

in Figs. 5.2 and 5.3. As the Reynolds number increases, the inertia force dominates the viscous force, and the friction factor decreases. Also, a greater number of coolant particles interact with the hot surface per unit of time and heat transfer rate due to convection enhancement. The dimensional parameters of the Tuckerman and Pease heat sinks are tabulated in Table 5.5. The various models have been suffixed as A, B, and C.

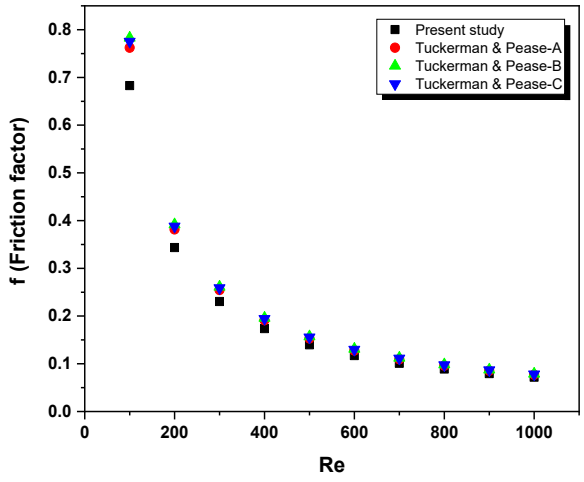

Fig. 5.2 Friction factor versus Reynolds number validation of the present model

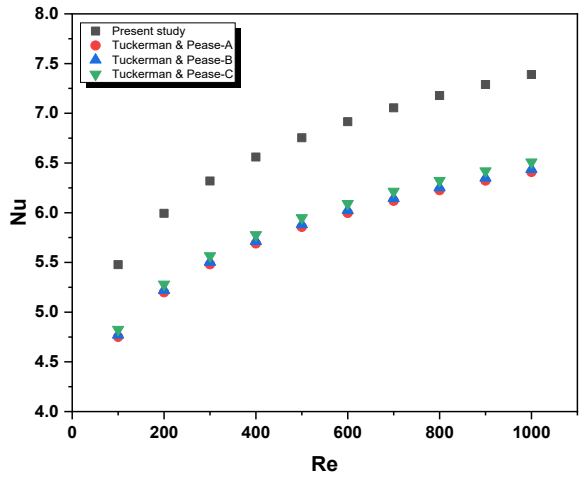

Fig. 5.3 Nusselt number versus Reynolds number validation of the present model

Table 5.5: Geometric specifications of the Tuckerman & Pease model used for validation

Parameters	Model A	Model B	Model C
H_c (mm)	0.287	0.302	0.320
w_c (mm)	0.055	0.05	0.056
w_w (mm)	0.045	0.05	0.044
t (mm)	0.143	0.256	0.213
D_h (mm)	0.0923	0.0858	0.0953

The friction factor of the different models confirms more precisely the present model at a high Reynolds number. However, the Nusselt number somewhat maintains a regular deviation for the Reynolds number variation from 100 to 1000. The difference in the hydraulic diameter of the different MCHS causes this variation in the values. For the validation process, water has been used as the coolant. On evaluation, the percentage variation in the friction factor of the present model is 8.4%, 10.74%, and 9.93% concerning models A, B, and C respectively. The deviation variations are 12.76% with model B and 6.39% with model A respectively. Similarly, the average variations in the Nusselt numbers are 15.29%, 14.87%, and 13.53%. Thus, a good agreement of the friction factors and Nusselt number values is found among different T and P models and the present model.

5.3 Results and Discussion

5.3.1 Heat transfer coefficient

The variation of the heat transfer coefficient with the volume flow rate for different coolants (i.e., water and hybrid nanofluid of dissimilar-shaped nanoparticles for φ=0.001) is shown in Fig. 5.4 (a). The coolant has been supplied at 25°C inlet temperature

as it was the room temperature measured at the time of the study. It is observed that the heat transfer coefficient increases with the volume flow rate. The hybrid nanofluids exhibit enhanced heat transfer coefficients due to increased thermal conductivity which is supported by Eq. (5.26) and pieces of literature. The cylindrical-brick (MWCNT-Fe_3O_4) shape blend shows the highest heat transfer coefficient throughout the variation of the volume flow rate. This shape blend is observed to have maintained an average heat transfer coefficient of 79.27% more than that of the water. The last enhancement is shown by the platelet-blade (graphene-Al_2O_3) shape blend which is 79.24% more than that of the water for the smallest volume flow rate. The rest of the blends possess relatively lower values of heat transfer coefficient than the cylindrical-brick (MWCNT-Fe_3O_4) blend. It is also found that the rate of increase of the parameter starts decreasing slowly as the volume flow rate of the coolant is increased. It may be because as the flow rate is increased, along with the introduction of the nanoparticles, the phenomena of Brownian motion is enhanced, and movement of the base fluid causes micro-convection around the nanoparticles. It happens because an increased volume flow rate enhances the Brownian motion and the micro-convection of the base fluid around the nanoparticles. The increase in volume concentration of the nanoparticles on the base fluid has been known to enhance the heat transfer coefficient.

Fig. 5.4 (b) shows that at a volume flow rate of 0.000004m^3/s and an inlet temperature of 25°C, the coefficient of heat transfer rises with the volume fraction of the nanoparticles. As the number of nanoparticles is increased in the base fluid, the number of nanoparticles carrying the heat in the mini channel increases, and the thermal transport properties of the coolant are improved. Among all the blends that have been studied, the cylindrical-brick (MWCNT-Fe_3O_4) shape blend exhibited the maximum heat transfer coefficient throughout the volume fraction variation.

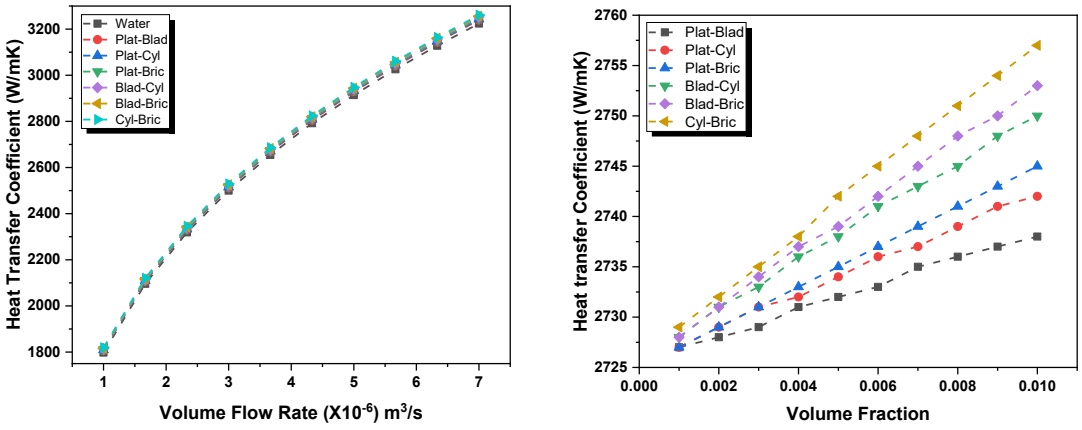

(a) **(b)**

Fig. 5.4 (a) Heat Transfer Coefficient v/s Volume Flow Rate (b) Heat Transfer Coefficient v/s Volume Fraction

This increment is about approximately 1.03% at φ=0.01 in comparison with that at φ=0.001 of the dissimilar-shaped nanoparticles hybrid nanofluid. However, is noticed that the coefficient increased by only 0.4% or 11W/m^{2}K for the platelet-blade blend. Also, it is noticeable, both in the case of volume flow rate and volume fraction variation, that any hybrid nanofluid blend consisting of the platelet shape performs relatively poorly in comparison to the rest of the blends in terms of the heat transfer coefficient. It may be because of the inefficient collision of the platelet-shaped nanoparticles with the other shapes that are being studied. However, it still exhibits better thermal characteristics than the base fluid i.e., water.

5.3.2 Nusselt number

With an increase in flow rate, the number of nanoparticles carrying away the heat from the channel surface increases. Thus, the Nusselt number, a dimensionless parameter that characterizes heat transfer increases with an increase in the volume flow rate of the working fluid. Fig. 5.5 (a) shows the same trend where the Nusselt number rises as the volume flow rate rises at φ=0.001 and inlet temperature of 25°C for the water-based,

dissimilar-shaped nanoparticles hybrid nanofluid. The variation trend of the Nusselt number is like that of the heat transfer coefficient when the volume flow rate is varied. As the volume flow rate is increased, the Reynolds number increases which is one of the major factors for the Nusselt number increment. The highest values of the Nusselt number are observed for the blade-brick blend which stays marginally higher than the cylindrical-brick blend. Initially, the Nusselt number value of the blade-brick blend is 1.74% higher than that of the water.

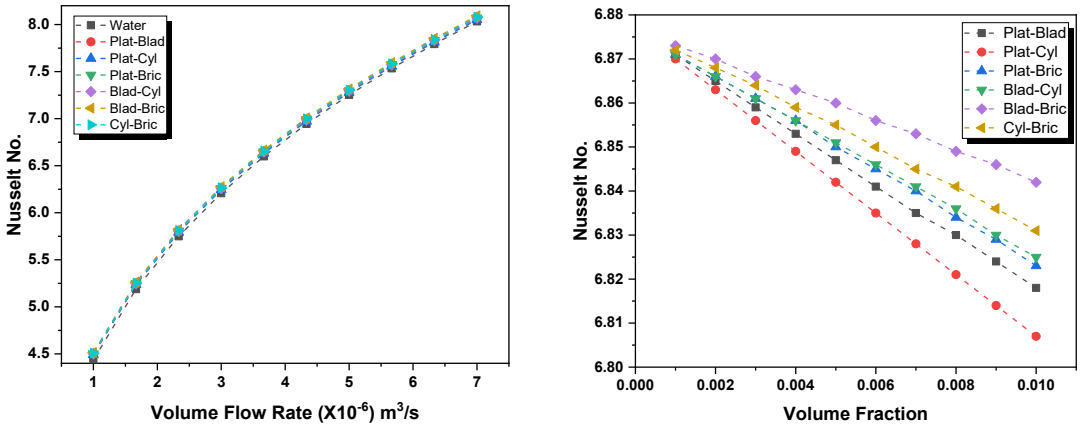

(a) **(b)**

Fig. 5.5 (a) Nusselt number v/s Volume Flow Rate (b) Nusselt number v/s Volume Fraction

However, as the flow rate is increased, this increment slowly diminishes to 0.75% at the flow rate of 0.000007m^3/s. The Nusselt number enhancement also implies that the convective heat transfer rate using a hybrid nanofluid also surges in comparison to the conductive heat transfer that occurs at the solid-liquid interface. The dispersing of dissimilar-shaped nanoparticles into the base fluid results in a trivial reduction in the Nusselt number as the volume fraction is increased. Fig. 5.5 (b) shows this fall at 25°C inlet temperature and 0.000004m^3/s volume flow rate of the different coolants. In the instance of similar particles, the particles tend to aggregate and form clusters that have

better heat transfer capabilities. This effect seemed to be lacking in the case of the combination of dissimilar nanoparticles. However, the negligible fall in the parameter is something that can be traded off in exchange for the faster cooling rate that comes along with the increase in the thermal conductivity of the coolants. This is because the addition of nanoparticles results in increased Brownian motion, rupture of the thermal boundary layer, and micro-convection. Talking about the shape effect of the nanoparticles, the blade-brick (Al_2O_3-Fe_3O_4) blend renders the best performance while the platelet-cylindrical (graphene-MWCNT) blend does not. The Nusselt number of the blade-brick blend reduces by 0.45% whereas, for the platelet-cylindrical blend, the reduction is 0.92%. A point that should be noted is that the brick shape presence enhances the heat transfer capabilities of the hybrid nanofluid. It might be due to the availability of surfaces of equal area on all sides which improves the efficiency of heat transfer due to better collision. A similar fall has been observed in a previous study.

5.3.3 Inlet and Outlet Exergy

Fig. 5.6 (a) shows the variation of the exergy at the inlet of the mini channel of the coolants against the volume flow rate at φ=0.001 and 25°C inlet temperature. Since the exergy directly depends on the coolant's mass flow rate, it rises as the volume flow rate rises. This variation has been reported before by authors. The exergy at the inlet is also a function of the temperature at the inlet of the mini channel and the ambient temperature. However, when the inlet temperature and the ambient temperature are fixed, the inlet exergy varies directly with the mass flow rate. Also, the different densities and heat capacities result in the discrete exergetic performance of the dissimilar-shaped nanoparticle hybrid nanofluid. From the figure, it can be ascertained that the blade-cylindrical (Al_2O_3-MWCNT) blend possesses the highest inlet exergy and increases by 1.044W. The blade-brick (Al_2O_3-Fe_3O_4) blend does not achieve fair exergetic

performance as it had been achieved in the thermal parameters. This might be due to better convective and conductive characteristics than capacitive ones. However, the rise in the exergetic opportunity is very close to that of the blade-brick blend i.e., 1.03 W for the blade-brick blend. The rise in the inlet exergy of the cylindrical-brick (MWCNT-Fe_3O_4) blend is also 1.044 W and it is next in the exergetic performance when compared to the blade-cylindrical blend.

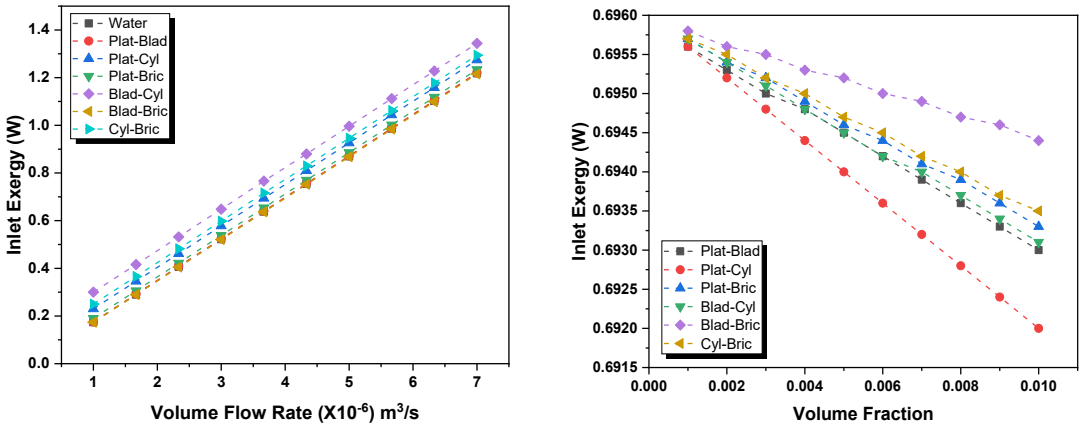

(a) **(b)**

Fig. 5.6 (a) Exergy at inlet v/s Volume Flow Rate (b) Exergy at inlet v/s Volume Fraction

With the increase in the proportion of the dissimilar-shaped nanoparticle in the coolant, the exergy at the inlet decreases, as can be observed from Fig. 5.6 (b). As the volume percentage of the different-shaped nanoparticle rises, the inlet exergy falls. The blade-brick shape blend exhibits the highest exergy while the platelet-cylindrical (graphene-MWCNT) shows the least. The minimum fall in the parameter is approximately 0.2% for the blade-brick blend.

The exergy at the outlet decreases as the volume flow rate increases. This is because as the volume flow rate is increased thermal entropy generation reduces due to a reduction in outlet temperature. Fig. 5.7 (a) shows the non-linear decrement of outlet

exergy as the volume flow rate is increased. The exergy at the outlet reaches negligible exergy because of a drastic fall in the outlet temperature, close to the ambient temperature. The exergy for blade-cylindrical (Al_2O_3-MWCNT) shape blend reduces by 25.7W while that for water decreases by 24.9W.

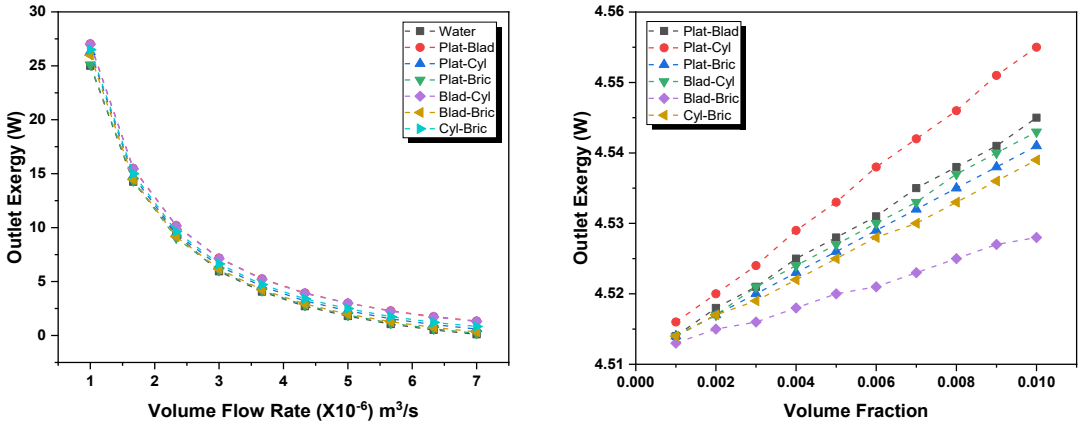

(a) **(b)**

Fig. 5.7 (a)Exergy at outlet v/s Volume Flow Rate (b) Exergy at outlet v/s Volume Fraction

Fig. 5.7 (b) shows the variation of outlet exergy with the change in volume fraction of the dissimilar-shaped nanoparticle hybrid nanofluids at 0.000004m^3/s and 25°C inlet temperature. The exergy at the outlet increases as the concentration of the particles increases. This is because the heat capacity of the coolant decreases with the introduction of the nanoparticles. The particles get heated up easily and so does the fluid surrounding the nanoparticles. The different shapes of the particles influence the heat transfer capabilities. Hence, this increment in the parameter is observed. Talking of the quantitative rise in the exergy at the outlet, it is 0.86% for the platelet-cylindrical shape blend, and 0.36% for the blade-brick shape blend.

5.3.4 Effect on the performance parameters

The coefficient of performance (COP) drops drastically as the volume flow rate is increased for both water and the hybrid nanofluid with φ=0.01 at 25°C inlet temperature as depicted in Fig. 5.8 (a). The COP of the heat sink applied with the hybrid nanofluid shows poor performance relative to water in terms of COP. This is because, for the removal of heat flux, the drop in pressure across the channel is more for the nanofluid. The dispersion of dissimilar-shaped nanoparticles to enhance thermal performance comes at the penalty of increased pressure drop or pumping power. The presence of nanoparticles increases the density and viscosity of the coolant which has been proved in many pieces of literature. The cylindrical-brick (MWCNT-Fe_3O_4) shape blend performs better than the other blends while the platelet-cylindrical combination exhibits the worst performance.

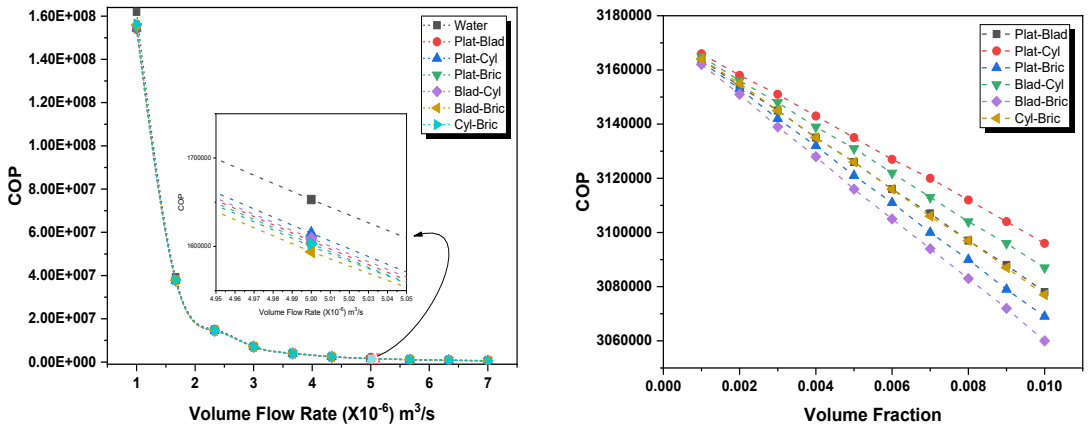

(a) **(b)**

Fig. 5.8 (a) COP v/s Volume Flow Rate (b) COP v/s Volume Fraction

However, at high flow rates, the COP of all the coolants converges which indicates that water is as good as any combination of articles at high volume flow rates. Fig. 5.8 (b) demonstrates the variation of COP with the volume fraction of dissimilar-shaped nanoparticle hybrid nanofluid from φ=0.001 to φ=0.01 at 25°C inlet temperature at a volume flow rate of 0.000004m^3/s. The COP of the mini channel heat sink applied with

the nanofluid for the given conditions and properties is observed to decrease with the increase in the volume concentration of nanoparticles. The platelet-cylindrical (graphene-MWCNT) shape blend exhibits the highest while the blade-brick (Al_2O_3-Fe_3O_4) shape blend shows the least COP among the combinations that are investigated in the study. The COP of platelet-cylindrical decreases by 2.21% and that of blade-brick decreases by 3.22%.

Fig. 5.9 (a) shows FOM variation with the volume flow rate of the coolant. As the flow rate increases, the Figure of merit increases. The enhancement is rapid in some of the dissimilar-shaped nanoparticle hybrid nanofluids. The ones possessing higher values initially do not exhibit much improvement while the ones with relatively smaller values show drastic increments. From close observation, the coolant with platelet shape nanoparticles in the blend showed a sudden increment. Also, the highest FOM is demonstrated by the blade-brick (Al_2O_3-Fe_3O_4) and the blade-cylindrical (Al_2O_3-MWCNT) shape blend at different flow rates. However, the highest enhancement is exhibited by the platelet-cylindrical (graphene-MWCNT) shape blend i.e., by 0.83%. Even though the Nusselt number is enhanced with the introduction of nanoparticles, pressure drop caused due to their presence hamper the FOM of the dissimilar-shaped hybrid nanofluid. As the volume flow rate increases, the Nu increases but still FOM value remains lower than 1 due to an overwhelming pressure drop.

The impact of the volume fraction variation of the dissimilar-shaped nanoparticles at 25°C inlet temperature and volume flow rate of 0.000004m^3/s is shown in Fig. 5.9 (b). The Figure of merit drops as the volume fraction of the nanoparticles increases.

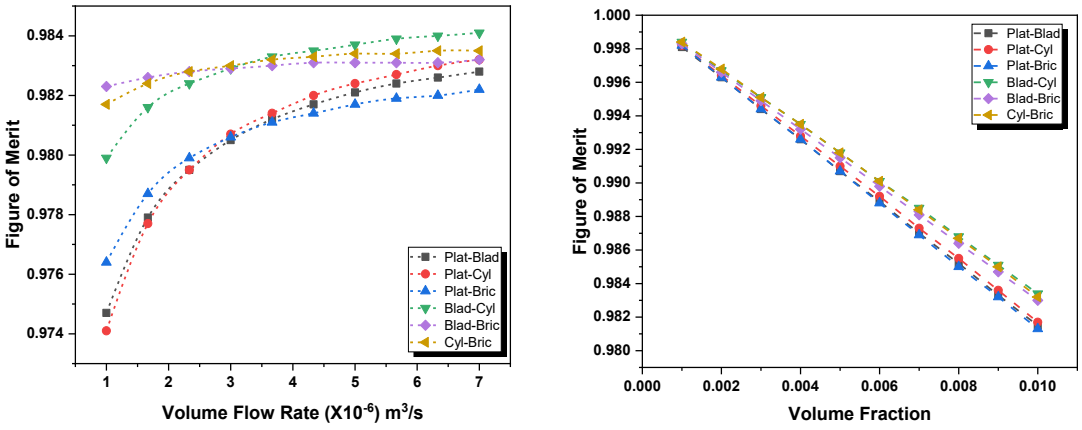

(a) **(b)**

Fig. 5.9 (a) Figure of Merit v/s Volume Flow Rate (b) Figure of Merit v/s Volume Fraction

It decreases by 1.5% for the blade-cylindrical (Al_2O_3-MWCNT) shape blend and by 1.69% for the platelet-brick (graphene-Fe_3O_4) blend. This is because the increase in the volume concentration of the nanoparticles of dissimilar shapes affects the hydraulic performance of the nanofluid adversely. It increases the density and viscosity of the coolant while decreasing its heat capacity. As a result, increased density and viscosity deteriorate the FOM of the hybrid nanofluid.

5.3.5 Effect on TEG performance

Fig. 5.10 (a) illustrates the relationship between the power output of a thermoelectric generator (TEG) and the volume flow rate of hybrid nanofluids. A distinct upward trend is observed, indicating that as the volume flow rate increases, the power output of the TEG also improves. This suggests that higher flow rates enhance the convective heat transfer, effectively maintaining a greater temperature gradient across the TEG, which directly contributes to increased power generation. Compared to water, which serves as the baseline coolant, all hybrid nanofluid formulations exhibit superior performance, demonstrating their enhanced thermal conductivity and heat transfer

capabilities. As the flow rate increases, the gap between different nanofluid formulations widens, indicating that at higher flow rates, the influence of nanoparticle shape on heat transfer becomes more pronounced. Fig. 5.10 (b) presents the relationship between the power output of a thermoelectric generator (TEG) and the volume concentration of hybrid nanofluids. A clear increasing trend is observed, indicating that as the volume concentration of nanoparticles increases, the power output of the TEG also rises. This suggests that higher nanoparticle concentrations enhance heat transfer, leading to more effective temperature differences across the TEG, which directly improves power generation. The highest TEG power and conversion efficiency is exhibited when a cylindrical-brick (MWCNT-Fe_3O_4) blend is used. The highest values obtained are 6.085W and 5.47% respectively.

Fig. 5.11 (a) illustrates the relationship between the conversion efficiency of a thermoelectric generator (TEG) and the volume flow rate of hybrid nanofluids. A clear trend is observed where the efficiency of TEG increases with an increasing flow rate for all the hybrid nanofluids tested. This trend suggests that higher flow rates enhance convective heat transfer, improving thermal management on the cold side of the TEG. Among the various hybrid nanofluids, platelet-brick (graphene-Fe_3O_4) and blade-brick (Al_2O_3-Fe_3O_4) exhibit the highest efficiency gains, outperforming all other combinations. These formulations likely benefit from the superior thermal conductivity and surface area effects of the brick-shaped nanoparticles, which enhance heat dissipation. Following closely behind, the blade-cylindrical (Al_2O_3-MWCNT) and cylindrical-brick (MWCNT-Fe_3O_4) blend also show significant efficiency improvements. On the other hand, the platelet-blade (graphene-Al_2O_3) hybrid nanofluid shows the least enhancement in conversion efficiency, performing only marginally better than water, which serves as the baseline coolant.

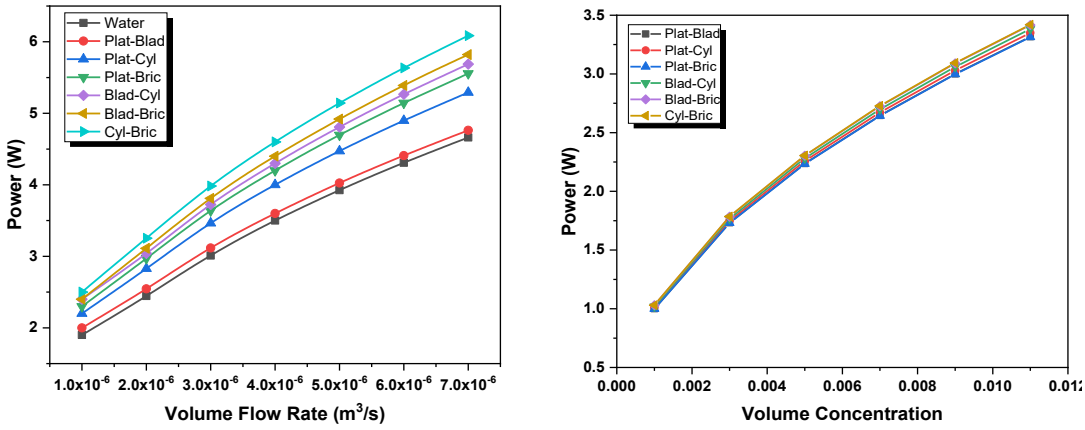

(a) **(b)**

Fig. 5.10 (a) TEG Power v/s Volume Flow Rate (b) TEG Power v/s Volume Fraction

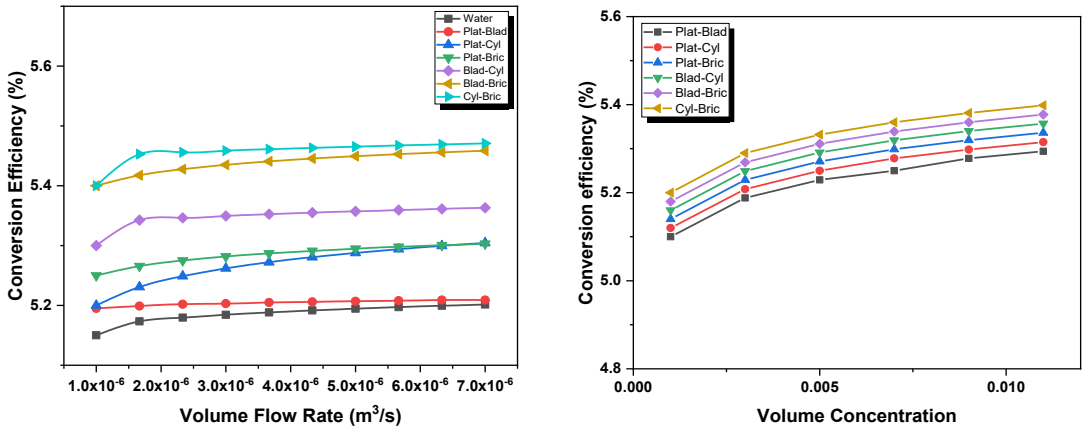

(a) **(b)**

Fig. 5.11(a) TEG conversion efficiency v/s Volume Flow Rate (b) TEG conversion efficiency v/s Volume Fraction

Fig. 5.11 (b) depicts the relationship between the conversion efficiency of a thermoelectric generator (TEG) and the volume concentration of hybrid nanofluids. A clear increasing trend is observed, where the TEG efficiency improves as the volume concentration of the nanofluid increases. This suggests that higher nanoparticle

concentrations contribute to enhanced thermal conductivity and improved convective heat transfer, resulting in better cooling on the cold side of the TEG. Among the tested hybrid nanofluids, the cylindrical-brick blend consistently achieves the highest efficiency across all volume concentrations, followed closely by the blade-brick (Al_2O_3-Fe_3O_4) and blade-cylindrical blend. These results indicate that incorporating brick-shaped nanoparticles significantly enhances the thermal performance, likely due to their high thermal conductivity and effective dispersion in the fluid.

5.4 Highlights

This research presents a novel investigation into the pivotal, yet underexplored, role of nanoparticle geometry in optimizing hybrid nanofluids for thermoelectric generator (TEG) cooling. Its primary contribution is a comprehensive evaluation of four distinct nanoparticle shapes (platelets, blades, cylinders, bricks) within a 50:50 hybrid mixture, providing deep insight into their synergistic effects on thermal-hydraulic performance and exergy dynamics. While employing established correlations, the innovative methodology lies in its systematic multi-parameter analysis, linking specific shapes to enhanced heat dissipation, improved coefficient of performance, and ultimately, significant gains in overall TEG power output and efficiency, surpassing conventional water or single-shape studies. The highlights are as follows:

- The average HTC increases with the increase in both volume flow rate and volume concentration due to an increase in thermal conductivity, relative motion between the nanoparticles, and micro-convection at the nanoparticle surface.
- The cylindrical-brick (MWCNT-Fe_3O_4) blend performs the best in terms of thermal properties with 79.27% enhancement with volume flow rate variation and 1.03% enhancement with the volume concentration.

- The blade-cylindrical (Al_2O_3-MWCNT) blend shows the best performance when the FOM is considered. The Figure of merit increases with the increase in the volume flow rate and the highest FOM observed is 0.9841.
- Also, a value of the Figure of merit lower than 1 for all the hybrid nanofluids is obtained.
- TEG power increases with volume flow rate due to increased cooling effect. Volume concentration increment enhances the TEG performance in terms of power and conversion efficiency.
- The highest TEG power and conversion efficiency are 6.085W and 5.47% respectively.
- Cylindrical-brick (MWCNT-Fe_3O_4) hybrid nanofluid gives the best TEG performance.